



# The temperature increase in Greenland has accelerated in the past five years

Saiping Jiang, Aizhong Ye\*, Cunde Xiao

State Key Laboratory of Earth Surface and Ecological Resources, Faculty of Geographical Science, Beijing Normal University, Beijing 100875, China



## ARTICLE INFO

### Keywords:

Temperature increase  
Teleconnection relationship  
Contribution rate  
Greenland

## ABSTRACT

Understanding the changes in Greenland's temperature is important for assessing and predicting the mass of the Greenland ice sheet, which plays an important role in sea level rise. In this study, we analyzed the annual and seasonal coastal Greenland's temperatures during the period 1952–2017 (focusing on the period 2013–2017) based on a dataset obtained from the Danish Meteorological Institute (DMI). Overall, the annual coastal Greenland's temperature increased during 1952–2017 at a rate of  $0.23\text{ }^{\circ}\text{C decade}^{-1}$ , especially in the south-eastern ( $0.70\text{ }^{\circ}\text{C decade}^{-1}$ ) and northern ( $0.42\text{ }^{\circ}\text{C decade}^{-1}$ ) regions of the island. From the changes in the seasonal coastal Greenland's composite temperature (CT), winter exhibited the largest change rate ( $0.28\text{ }^{\circ}\text{C decade}^{-1}$ ), and the summer CT increased by  $0.25\text{ }^{\circ}\text{C decade}^{-1}$ , while the spring CT increased by  $0.17\text{ }^{\circ}\text{C decade}^{-1}$  with less variation. The temperature increase accelerated during 2013–2017 according to Mann-Kendall (M-K) tests, especially in the northeastern and northern regions of the island. The seasonal temperature change of the whole island decreased in the following order: annual > autumn > summer > winter > spring. We also analyzed the annual inland temperature change during the period 1997–2017 based on a dataset obtained from the Greenland Climate Network; the results indicated that the inland temperature increased by  $0.13\text{ }^{\circ}\text{C decade}^{-1}$ . Pearson correlation analysis was used to determine the teleconnection relationship between the coastal temperatures and large-scale atmosphere-ocean climate indexes, and we found that the Greenland Blocking Index (GBI), Atlantic Multidecadal Oscillation (AMO), Tropical Northern Atlantic Index (TNA), North Tropical Atlantic Index (NTA), Caribbean Index (CAR), Atlantic Meridional Mode (AMM), East Atlantic (EA) and Western Hemisphere warm pool (WHWP) have significant positive correlations with the coastal temperature in most months, except in February and May. However, the North Atlantic Oscillation (NAO), Arctic Oscillation (AO) and Eastern Asia/Western Russia (EAWR) show significant negative correlations with temperature. Overall, there exists a time lag effect between the climate indexes (except for the GBI, AO and NAO) and temperature. From the application of the random forest model, we found that the GBI, NAO,  $\text{CO}_2$ , AMO,  $\text{N}_2\text{O}$ ,  $\text{SF}_6$ ,  $\text{CH}_4$ , and Northern Oscillation Index (NOI) are the most important variables that influenced the CT changes during 1979–2017. Finally, we calculated the contribution rates of the most important variables to temperature change during the period 1979–2017 and showed that the contribution rates of the GBI,  $\text{CO}_2$  and NOI to temperature change were 47.30%, 35.68%, and 17.02%, respectively.

## 1. Introduction

Greenland is a particularly salient example of temperature change resulting in polar amplification (Johannessen et al., 2004; Polyakov et al., 2002). Eighty-two percent of the island is covered by ice and snow, which is sensitive to climate change and plays an important role in rising sea levels (Cuffey and Marshall, 2000; Hvidberg, 2000).

The change in Greenland's temperature at the centennial scale is important and has received much attention (Vinther et al., 2006; Hanna et al., 2012). Studies on this topic mainly focus on two aspects. On the

one hand, some studies concentrate on determining the change trend of Greenland's temperature. For instance, Box (2002) analyzed the variation in Greenland's temperature during the period 1873–2001 and found that the Greenland's temperature increased during the periods 1885–1947 and 1984–2001 and decreased during the period of 1955–1984. Additionally, warming of  $2\text{--}4\text{ }^{\circ}\text{C}$  occurred in the western region of Greenland during the period 1991–2000. According to long time-series records, the Greenland coastal temperature decreased by  $1.29\text{ }^{\circ}\text{C}$  during the period 1958–2001 (Hanna and Cappelen, 2003). Subsequently, Box et al. (2009) extended the temperature records to

\* Corresponding author at: State Key Laboratory of Earth Surface and Ecological Resources, Faculty of Geographical Science, Beijing Normal University, Beijing 100875, China.

E-mail address: [azyebnu@bnu.edu.cn](mailto:azyebnu@bnu.edu.cn) (A. Ye).

<https://doi.org/10.1016/j.gloplacha.2020.103297>

Received 22 January 2020; Received in revised form 9 August 2020; Accepted 18 August 2020

Available online 25 August 2020

0921-8181/ © 2020 Elsevier B.V. All rights reserved.

2007 and found that during the period 1840–2007, only the temperature in 2003 was anomalously high compared with the temperature during the base period 1951–1980, and the warming of 1994–2007 was within the envelope of the Northern Hemisphere anomaly compared with the warming observed during the 1920s. On these bases, Hanna et al. (2012) updated the analysis to 2012 mainly to analyze the temperature variation during the period 1991–2011 and found strong warming in Greenland over the previous 20 years, especially in winter and the western region of the island, where the warming exceeded 10 °C. In addition, Mernild et al. (2014) analyzed the temperature extremes in coastal Greenland during the period 1890–2010 and found that the 2000s and 1890s had the highest numbers of days with warm and cold extremes, respectively. The number of days with warm extremes in the 2000s was approximately 50% higher than that in the 1940s. Furthermore, the Danish Meteorological Institute (DMI) updates the Greenland's temperature records on its official website every year, thereby offering a convenient basis for research on the temperature change in Greenland. On the other hand, some scholars have tried to interpret the reasons responsible for Greenland's temperature change. They found that North Atlantic Oscillation (NAO), Greenland Blocking Index (GBI), Atlantic Multidecadal Oscillation (AMO), tropical forcing, sea ice albedo feedback and greenhouse gases (GHGs) are the most important factors influencing changes in Greenland's temperature (Chylek et al., 2004; Hanna et al., 2016; Ding et al., 2014; Graversen et al., 2008; Chylek et al., 2009).

However, we must ask the following question: what if the Greenland's temperature keeps increasing during the period 2013–2017? According to the Statement on global climate published by World Meteorological Organization (WMO) in 2017, the year of 2013–2017 was the warmest five years since 1900 on record; moreover, the mean temperature of these five years was 0.4 °C higher than the 1981–2010 average (and 1.0 °C higher than the preindustrial values). This report also indicated that during 2013–2017, the Arctic experienced the strongest warming in the world (World Meteorological Organization, 2018). Moreover, what if other climate indexes influence the change in Greenland's temperature? Examples of such indexes include the El Niño-Southern Oscillation (ENSO) index, Caribbean Index (CAR), Northern Oscillation Index (NOI) and so on (Hidalgo-Muñoz et al., 2015; Penland and Matrosova, 1998; Schwing et al., 2002). Finally, how much do changes in GHGs and climate indexes contribute to temperature change? The answers to all of these questions remain unknown.

Therefore, in this paper, we aim to address three questions: (1) How did the Greenland's temperature change during the period 2013–2017? (2) Do other climate indexes and variables play important roles in influencing Greenland's temperature? (3) What are the contribution rates of important variables to changes in Greenland's temperature? Answering these questions will provide support for future research on climate change and sea ice prediction.

The organization of the remainder of this paper is as follows: Section 2 describes the methods, including the Mann-Kendall (M-K) test, Pearson correlation analysis, random forest model and multiple linear regression; Section 3 introduces the study area and data sources; Section 4 presents the results and discussion; and Section 5 provides the conclusions.

## 2. Method

In this study, we used the M-K test to determine the Greenland's temperature change trend, and we employed Pearson correlation analysis to measure the linear correlations between the temperature and various climate indexes and GHGs. We also used the random forest model to calculate the sensitivity of variables to temperature change. Finally, we used multiple linear regression to calculate the contribution rates of climate indexes and GHGs to temperature change.

### 2.1. Mann-Kendall test

The M-K test is a nonparametric statistical method proposed and developed by Mann (1945) and Kendall (1948). The M-K test does not require samples to follow a certain distribution and is not disturbed by a few outliers; hence, this approach has been widely recommended by the World Meteorological Organization (WMO) for the determination of climatic and hydrologic data change trends in time series (Mitchell et al., 1966).

For observational data in a time series, namely,  $X = x_1, x_2, \dots, x_n$ , Eq. (1) and Eq. (2) are used to calculate the M-K trend statistic (S). In this study, we directly employed original temperature data to analyze the change trend because the autocorrelation coefficient of the temperature data did not pass the significance test at a level of 0.05. And in the following text, all “pass the significance test” means “at the level 0.05”. The standardized MK statistic Z is used to determine the change trend of observational data in a time series if the number of observations, n, is sufficiently large ( $n > 10$ ). Here, we used Eq. (3), Eq. (4) and Eq. (5) to compute the Z value, where E(S) and Var(S) represent the expected value and variance of S, respectively.

A Z value greater than zero indicates that the data in a time series display an increasing trend; if the Z value equals zero, the data in a time series remain steady; and a Z value less than zero indicates that the data in a time series exhibit a decreasing trend. If  $|Z| \geq Z_{(1-\alpha/2)}$ , the data in a time series have a significantly increasing or decreasing trend under a significance level  $\alpha$ . Absolute values of Z greater than or equal to 1.28, 1.96 and 2.23 indicate that the data in time series pass significance tests at levels of 0.1, 0.05, and 0.01, respectively.

$$S = \sum_{i=1}^{n-1} \sum_{j=i+1}^n \text{sign}(x_j - x_i) \quad (1)$$

$$\text{sign}(x_j - x_i) = \begin{cases} 1, & x_j > x_i \\ 0, & x_j = x_i \\ -1, & x_j < x_i \end{cases} \quad (2)$$

$$Z = \begin{cases} \frac{S - 1}{\sqrt{\text{Var}(S)}}, & S > 0 \\ 0, & S = 0 \\ \frac{S + 1}{\sqrt{\text{Var}(S)}}, & S < 0 \end{cases} \quad (3)$$

$$E(S) = 0 \quad (4)$$

$$\text{Var}(S) = \frac{n(n-1)(2n+5)}{18} \quad (5)$$

### 2.2. Pearson correlation analysis

In this study, we used Pearson correlation analysis to measure the linear correlations between the temperature and various climate indexes and GHGs.

$$R = \frac{\sum_{i=1}^n (X_i - \bar{X})(Y_i - \bar{Y})}{\sqrt{\sum_{i=1}^n (X_i - \bar{X})^2} \sqrt{\sum_{i=1}^n (Y_i - \bar{Y})^2}} \quad (6)$$

where, R represents the Pearson correlation coefficient between X and Y, where 1, -1 and 0 reflect a completely positive correlation, a completely negative correlation and no correlation, respectively, between X and Y. The t-test method was used to determine the significance of the correlation coefficient.  $X_i$  and  $Y_i$  reflect the variable values in year i, and  $\bar{X}$  and  $\bar{Y}$  are the corresponding mean values.

### 2.3. Random forest model

The random forest model is an ensemble learning method proposed

by Breiman, 2001, that is suitable for both classification and regression problems. This model generates a new training set by randomly selecting  $M$  samples from the original dataset using the bootstrap resampling technique, and then a random forest is generated by the new training set. The units unselected in each iteration constitute  $M$  out-of-bag data, namely, the OOB error (Breiman, 2001). The number of variables for the splitting node ( $m_{try}$ ) and the number of trees ( $n_{tree}$ ) are important elements for the random forest model. The value of one-third of all variables is the default  $m_{try}$  value in a regression problem; sometimes, the model selects the default value, one-half of the default value or twice the default value as the  $m_{try}$  value (Liaw and Wiener, 2002). The  $n_{tree}$  value is usually set as 500, 1000, 1500 or 2000. The parameter combination that minimizes the OOB error of the model is selected for the final prediction. In this study,  $m_{try}$  was selected as 15, and  $n_{tree}$  was chosen to be 500. And we used mean error (ME), root mean square error (RMSE) and decision coefficient  $R^2$  to evaluate the accuracy of the prediction. When ME is close to zero, it indicates that the method is unbiased, and the RMSE is smaller, the accuracy of the model is higher.  $R^2$  represents the explanatory ability of the model to the dependent variable.

#### 2.4. Multiple linear regression

In this study, we used multiple linear regression to calculate the contribution rates of climate indexes and GHGs to temperature change:

$$Y = a + b_1x_1 + b_2x_2 + \dots + b_nx_n + \varepsilon_i \quad (7)$$

where  $x_n$  represents the  $n$ th independent variable,  $Y$  represents the dependent variable,  $a$  is the constant, and  $\varepsilon_i$  is the random error.

We used stepwise regression method to fit the regression equation, and the probability of “F-to enter” and “F-to move” is 0.05 and 0.1, respectively. And Variance Inflation Fraction (VIF) was used to check the multicollinearity, when  $\sqrt{vif} > 2$ , it means that the regression equation exists multicollinearity. In order to avoid the multicollinearity, we sorted the variables that are significantly correlated with the Greenland composite temperature (CT), and the variable with the largest correlation coefficient was selected first. If another variable had a correlation coefficient within 0.5 with a previously selected variable, the variable was selected; otherwise, the variable was abandoned. Finally, we used the selected variables to build multiple linear regression equation, and AIC value was used to select which variable should be retained and which variable should be removed in the equation, the variables that make the AIC value smallest are in the final equation.

We used the multiple linear regression to calculate the contribution rate of important variables to CT change during 1979–2017. And we divided the period into two parts, namely, period 1979–1998 and period 1999–2017, then we calculated the mean value of CT and important variables in two periods, respectively. The CT change is the mean value during period 1999–2017 minus the mean value during period 1979–1998, namely, temperature change (TC). When we calculate one variable to the contribution rate of CT change, the other variables remain steady. The mean value of the variable during period in 1999–2017 and the mean value of other variables during period 1979–1998 were used in the multiple linear regression equation to predict the temperature, then we used the predicted temperature minus the mean CT during period 1979–1998, namely, the temperature change caused by the variable changes ( $TC_n$ ).  $TC_n$  divided by TC and multiply 100 is the contribution rate of one variable to CT change. Because TC is the observed temperature change value, and  $TC_n$  is temperature change caused by one variable changes, which was calculated by model, there exists residual between actual value and predicted value. Total contribute of important variables to temperature change may be not 100%. In order to avoid this situation, the contribution rate of each variable is divided by total contribution rate calculated by model, namely, relative contribution rate, as the contribution rate of each variable to temperature change.

### 3. Study area and data

#### 3.1. Study area

Greenland is the largest island in the world with a total area of 2,166,086 km<sup>2</sup>. Eighty-two percent of the island is covered by an ice sheet. The coastline stretches 44,087 km, and the largest north-south and east-west distances are 2670 and 1050 km, respectively. The population of Greenland is 555,877 people (from a statistical study in 2018), most of whom live on the southwestern part of the island. Three-quarters of Greenland is located in the Arctic, and the northern part of the island experiences a High Arctic climate; the annual temperature is below  $-12$  °C. The middle and southern parts of the island have a Low Arctic climate. The deep fiords on the southern part of the island have a sub-Arctic climate, and the agriculture consists mainly of sheep farming. The fishing industry is the main source of income for the island, accounting for 80% of the total output of export commodities. Greenland is bounded by the Arctic Ocean to the north, the Greenland Sea to the east, the North Atlantic Ocean to the southeast, the Davis Strait to southwest, and Baffin Bay to the west. Because Greenland is near the ocean, the Greenland's climate is easily influenced by sea currents. Arctic Ocean and North Atlantic Ocean sea currents affect the exchanges of heat and cold with the island. Five hydropower plants have been built to supply energy since the 1990s. Before this, fossil fuels were the main energy source. Some small towns still rely on fossil fuels to produce electricity. Hotel guests by nationality rose from 44,270 to 63,393 during the period 2013–2017 (Statistics Greenland, 2018).

#### 3.2. Observed temperature data

##### 3.2.1. Coastal air temperature data

The observed Greenland monthly mean coastal surface air temperature (SAT) data were obtained from the DMI (online at <https://www.dmi.dk/publikationer/>). A total of 14 weather station sites from coastal Greenland were collected in this study, which have SAT records spanning the same period (from 1952 to 2017). And the data missing proportion is 2–6% except 4301 station, which is 14%. And we used the linear regression methods to fill the gaps. Four steps were considered. First, we used raw monthly mean coastal SAT data from Greenland downloaded from Berkeley Earth (BE) (online at <http://berkeleyearth.org/>) to fill the gaps, and linear regression was used to adjust the ‘baseline’ DMI data. Note that all the correlation coefficients between the DMI coastal SAT data and BE raw coastal SAT data are above 0.75. Second, if BE raw coastal SAT data were also missing, we first used expected BE regional coastal temperature data to predict the BE raw coastal SAT data, and then the predicted BE raw coastal SAT data were used to supplement the DMI coastal SAT data. Third, if the expected BE regional coastal temperature data were also missing, we computed the DMI monthly mean coastal temperatures for the two years adjacent to the missing data to fill the gaps. Fourth, if there were missing values for more than 2 years in the dataset, we used the sites adjacent to the DMI data to fill the gaps, which were adjusted by elevation information, namely, the temperature decreases 0.65 °C for elevation increases every 100 m. We divided the island into six coastal regions to analyze the temperature change in each area; Fig. 1 shows the spatial distribution of the 14 weather stations and the boundaries of the six coastal regions. In addition, we also constructed the Greenland composite temperature (CT) for the coastal SAT records from 1952 to 2017 to analyze the whole temperature change trend among the Greenland's coastal regions.

In this study, we analyzed annual and seasonal temperature changes. We averaged the temperature data from all twelve months every year to obtain the annual temperature data. The standard three-month meteorological seasons, namely, DJF (winter), MAM (spring), JJA (summer), and SON (autumn), were used in this study. Finally, we

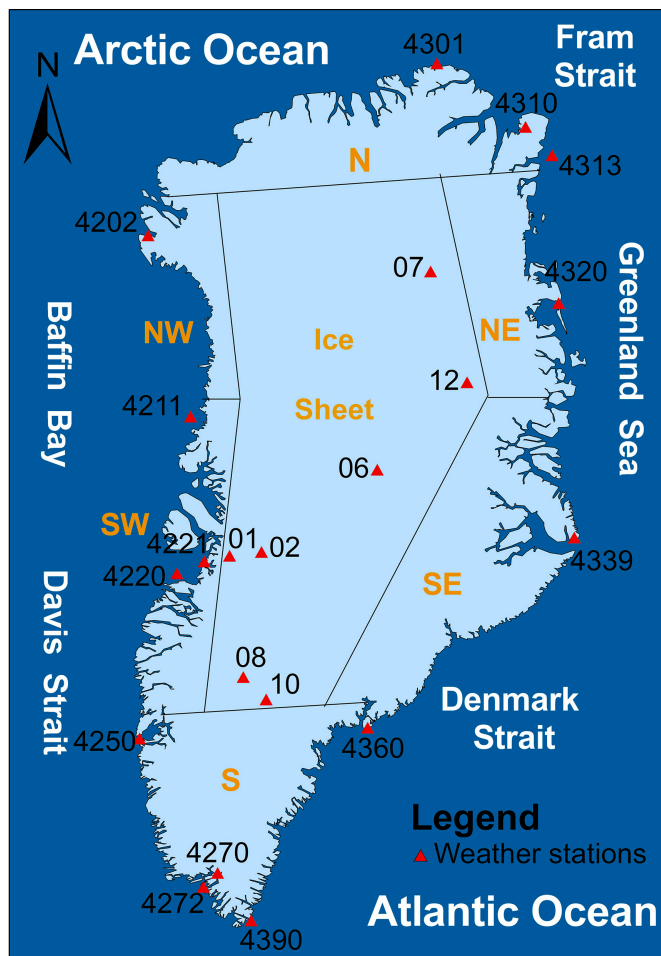


**Fig. 1.** Location map of weather stations and climate regions. The weather stations are 4301 Kap Morris Jesup, 4310 Station Nord, 4313 Henrik Krøyer Holme, 4320 Danmarkshavn, 4339 Ittoqqortoormiit, 4360 Tasiilaq, 4390 Ikerassuaq, 4272 Qaqqortoq, 4270 Mitt. Narsarsuaq, 4250 Nuuk, 4220 Aasiaat, 4221 Mitt. Ilulissat, 4211 Mitt. Upernavik, 4202 Pituffik, 07 TUNU-N, 12 NASA-E, 06 Summit, 01 Swiss Camp, 02 Crawford Pt., 08 Dye-2, 10 Saddle. Data from 10 (Saddle) and 02 (Crawford Pt.) were used to fill the gaps of 08 (Dye-2) and 06 (Summit), respectively. N, NW, NE, SE, SW and S represent the northern, northwestern, northeastern, southeastern, southwestern and southern coastal regions of the island, respectively.

used temperature anomalies relative to the 1981–2010 baseline climatology.

**3.2.2. Inland air temperature data**

Air temperature data from the inland territory of Greenland were collected from the Greenland Climate Network (GC-Net; see Steffen et al., 1996; Steffen and Box, 2001). We collected data from seven stations (Fig. 1), but stations 10 (Saddle) and 02 (Crawford Pt.) were mainly used to fill the gaps of 08 (Dye-2) and 06 (Summit), respectively. The other five stations provided air temperature records from 1997 to 2017. The completeness of the data from these five stations is greater than 76%. It should be noted that some gaps were filled by adjacent stations and the mean values of adjacent years, which may introduce some bias compared with the true temperature. We averaged the annual surface air temperatures at these five stations as the inland temperature (IT) to determine the temperature change over the past 21 years.

**3.3. Atmospheric and ocean climate index data**

The NAO and ENSO are two important teleconnection patterns influencing the global climate (Hidalgo-Muñoz et al., 2015). Some researchers have found that the NAO has a negative correlation with the Greenland’s temperature (Box, 2002; Hanna et al., 2012), which affects the Greenland’s climate. The ENSO Sea Surface Temperature (SST) variability originates from the Pacific but can extend to the tropical Atlantic due to the time lag effect (Mestas-Nunez and Enfield, 2001); this variability influences the climate at the global scale (Hidalgo-Muñoz et al., 2015). There are other teleconnection patterns that affect the Arctic climate, such as the GBI, Arctic Oscillation (AO) (Hanna et al., 2015) and AMO (Chylek et al., 2009). Hidalgo-Muñoz et al. (2015) reviewed many teleconnection indexes, including the AO, NAO, AMO, East Atlantic (EA), Eastern Asia/Western Russia (EAWR), Southern Oscillation Index (SOI), Western Pacific pattern (WP), East Pacific-North Pacific pattern (EP-NP), Pacific North Atlantic (PNA), and Pacific Decadal Oscillation (PDO), and indicated that these indexes affect climate change in the Iberian Peninsula. Greenland is surrounded by sea, and thus, the island is easily affected by sea currents. On these bases, in this study, we selected twenty-eight large-scale atmospheric and ocean climate indexes distributed throughout the Arctic Ocean, the Atlantic Ocean, the Pacific Ocean and the Indian Ocean to find the most important variables affecting the Greenland’s temperature. The variables are listed in Table 1.

The monthly atmospheric and ocean time-series climate index data were downloaded from the National Oceanic Atmospheric Administration (NOAA) (online at <https://www.esrl.noaa.gov/psd/data/climateindexes/list/>) except for the GBI data, which were obtained from Hanna et al. (2015) at the following website: <https://www.>

**Table 1**  
Description of large-scale monthly climate indexes.

Climate index	Description	Location
NAO	North Atlantic Oscillation	North Atlantic
AMO	Atlantic Multidecadal Oscillation	Atlantic
AO	Arctic Oscillation	Arctic Region
AAO	Antarctic Oscillation	40–65°S
AMM	Atlantic Meridional Mode	Tropical Atlantic
NTA	North Tropical Atlantic Index	5–25°N, 15–60°W
TNA	Tropical Northern Atlantic Index	5–25°N, 15–55°W
TSA	Tropical Southern Atlantic Index	0–20°S, 10°E ~ 30°W
CAR	Caribbean Index	Caribbean Sea
EA	East Atlantic	North Atlantic
EAWR	Eastern Asia/Western Russia	North Atlantic/Eurasia (20–90°N)
GBI	Greenland Blocking Index	60–80°N, 20–80°W
PDO	Pacific Decadal Oscillation	North Pacific (20–90°N)
PNA	Pacific North American Index	Northern Hemisphere (20–90°N)
QBO	Quasi-Biennial Oscillation	Tropical stratosphere
WP	Western Pacific Index	25–40°N (50–70°N), 140°E ~ 150°W
NP	North Pacific Pattern	30–65°N, 160°E ~ 140°W
WHWP	Western Hemisphere Warm Pool	Atlantic and North ~ East Pacific
NOI	Northern Oscillation Index	North Pacific High and near Darwin Australia
MEI	Multivariate ENSO Index	Tropical Pacific
BEST	Bivariate ENSO Time Series	Tropical Pacific
Nino3	Eastern Tropical Pacific (SST)	5°N ~ 5°S, 150–90°W
Nino4	Central Tropical Pacific (SST)	5°N ~ 5°S, 160°E ~ 150°W
Nino1 + 2	Extreme Eastern Tropical Pacific	0–10°S, 90–80°W
Nino3.4	East Central Tropical Pacific (SST)	5°N ~ 5°S, 170–120°W
ONI	Oceanic Nino Index	5°N ~ 5°S, 170–120°W
SOI	Southern Oscillation Index	Tropical Pacific
TNI	Trans-Nino Index	0–10°S, 90–80°W; 5°N ~ 5°S, 160°E ~ 150°W

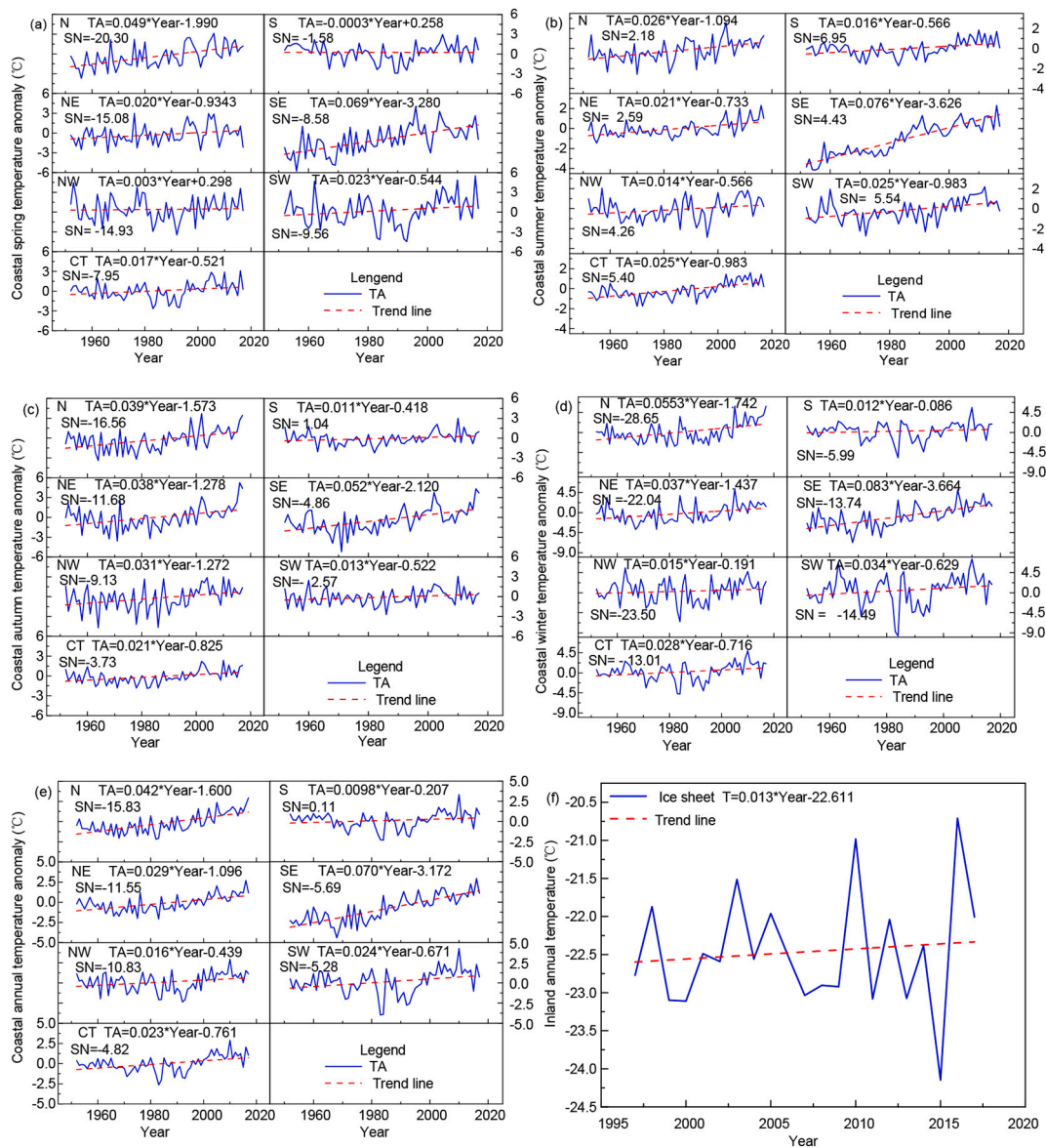


**Fig. 2.** Greenland surface air temperature changes during 1952–2017. Each relationship between the temperature and year was built using linear regression, and the climate tendency rate, which is defined as the slope of the regression equation multiplied by ten, was used to describe the Greenland's temperature change every decade. SN is the standard normal value which represents the average temperature during the period 1981–2010, and TA is the temperature anomaly relative to the 1981–2010 mean temperature. The eastern region includes the northeastern and southeastern coastal regions of the island, and the western region includes the northwestern and southwestern coastal regions of the island.

[esrl.noaa.gov/psd/gcos\\_wgsp/Timeseries/GBI\\_UL/](https://www.esrl.noaa.gov/psd/gcos_wgsp/Timeseries/GBI_UL/).

### 3.4. Greenhouse gas (GHG) data

We used annual GHG data (1979–2017) to analyze the influence of GHGs on the temperature change in Greenland. The dataset was obtained from NOAA (online at <https://www.esrl.noaa.gov/gmd/ccgg/aggi.html>).

### 3.5. Sea ice data

We also used monthly sea ice area data from the Northern Hemisphere to help interpret the Greenland's temperature changes. The data are available at the National Snow & Ice Data Center (NSIDC) (online at [https://nsidc.org/data/seaice\\_index/archives](https://nsidc.org/data/seaice_index/archives)).

## 4. Results and discussion

### 4.1. Temperature variation during the period 1952–2017 in Greenland

Fig. 2 shows the seasonal and annual temperature changes of the coastal regions across the island during the period 1952–2017. The temperatures in 1983/84 and 1992 were unusually cold, which may be linked to the 1983 El Chichón eruption and the 1991 Mt. Pinatubo eruption (Abdalati and Steffen, 1997; Box, 2002).

As seen from Fig. 2a, the mean coastal spring temperatures in different regions during 1952–2017 range from  $-1.33$  in the southern region to  $-20.66$  °C in the northern region, and the mean spring CT is  $-7.9$  °C ( $0.05$  °C higher than the SN ( $-7.95$  °C)). It is obvious that the temperature in the northern region of the island is lower than that in the southern region due to the different Arctic climates, while there is little difference in the temperature between the eastern region and the western region of the island. The climate tendency rate indicates that

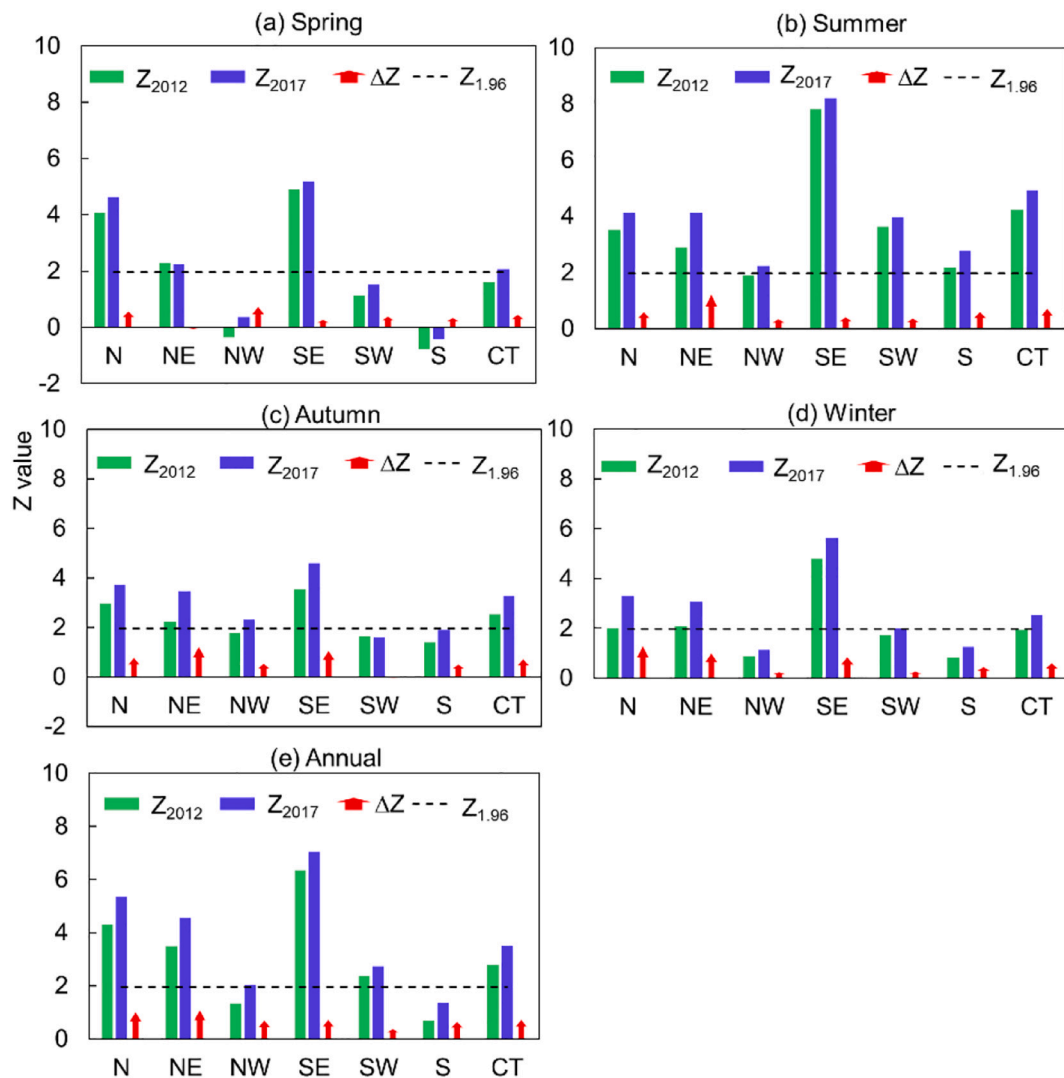


**Fig. 3.** M-K test values of the coastal temperatures in Greenland.  $Z_{2012}$  and  $Z_{2017}$  represent the Z values according to the M-K test results during the periods 1952–2012 and 1952–2017, respectively.  $\Delta Z$  is the value of the change in Z during the period 2013–2017, namely, the Z value of the period 1952–2017 minus the Z value of the period 1952–2012. A value of  $\Delta Z$  greater than 0 indicates that the coastal temperature increased during 2013–2017, and vice versa.  $Z_{1.96}$  represents a 0.05 significance level.

the temperature in most regions has risen during the period 1952–2017, except in the southern and northwestern regions, where the temperature has remained nearly steady. The order of the climate tendency rate among the different regions ( $SE > N > SW > NE > NW > S$ ) shows that the temperature change in the eastern region has been more dramatic than that in the western region, especially in the southeastern region of the island, where the temperature change trend is  $0.69\text{ }^{\circ}\text{C decade}^{-1}$  and the CT increases by  $0.17\text{ }^{\circ}\text{C decade}^{-1}$ . Additionally, the temperature change trend is larger in the northern region than in the southern region.

Fig. 2b shows the coastal summer temperature changes during the period 1952–2017, illustrating that the mean summer temperature in all coastal regions of the island is above  $0\text{ }^{\circ}\text{C}$ , and the mean summer CT is  $5.24\text{ }^{\circ}\text{C}$  ( $0.16\text{ }^{\circ}\text{C}$  lower than the SN ( $5.40\text{ }^{\circ}\text{C}$ )). There exists a large temperature difference of  $4.99\text{ }^{\circ}\text{C}$  between the northern and southern regions, while the temperature difference between the eastern and western regions is below  $2.03\text{ }^{\circ}\text{C}$ . The order of the climate tendency rate in summer ( $SE > N > SW > NE > S > NW$ ) indicates an increasing temperature change trend in all regions during 1952–2017; among them, the southeastern region has the largest temperature change trend of  $0.76\text{ }^{\circ}\text{C decade}^{-1}$ , and the CT increases by  $0.25\text{ }^{\circ}\text{C decade}^{-1}$ .

The coastal autumn temperature changes during 1952–2017 are shown in Fig. 2c. The warmest mean temperature is  $0.998\text{ }^{\circ}\text{C}$  in the southern region of the island, while the coldest mean temperature is  $-16.84\text{ }^{\circ}\text{C}$  in the northern region. Moreover, it is  $2.33\text{--}2.6\text{ }^{\circ}\text{C}$  colder in the eastern region than in the western region of the island, and the coastal autumn CT is  $-3.85\text{ }^{\circ}\text{C}$  ( $0.12\text{ }^{\circ}\text{C}$  lower than the SN ( $-3.73\text{ }^{\circ}\text{C}$ )). From the order of the climate tendency rate ( $SE > N > NE > NW > SW > S$ ), we can see that all the values are above 0, indicating that an increasing temperature change trend may have existed during the period 1952–2017. It is obvious that the temperature has the fastest increasing trend in the southeastern region, where the temperature change trend is  $0.52\text{ }^{\circ}\text{C decade}^{-1}$ , and CT rises at a rate of  $0.21\text{ }^{\circ}\text{C decade}^{-1}$ .

Fig. 2d shows that the mean coastal winter temperature ranges from  $-28.54\text{ }^{\circ}\text{C}$  in the northern region to  $-5.69\text{ }^{\circ}\text{C}$  in the southern region during the period 1952–2017, and the mean winter CT is  $-12.79\text{ }^{\circ}\text{C}$  ( $0.22\text{ }^{\circ}\text{C}$  lower than the SN ( $-13.01\text{ }^{\circ}\text{C}$ )). It is evident that the temperature in the western region is much higher than that in the eastern region, and the difference in temperature between these two regions ranges from  $7.62$  to  $9.19\text{ }^{\circ}\text{C}$ . Regarding the order of the climate tendency rate ( $SE > N > NE > SW > NW > S$ ), all regions seem to display a warming trend during the period 1952–2017; among them,

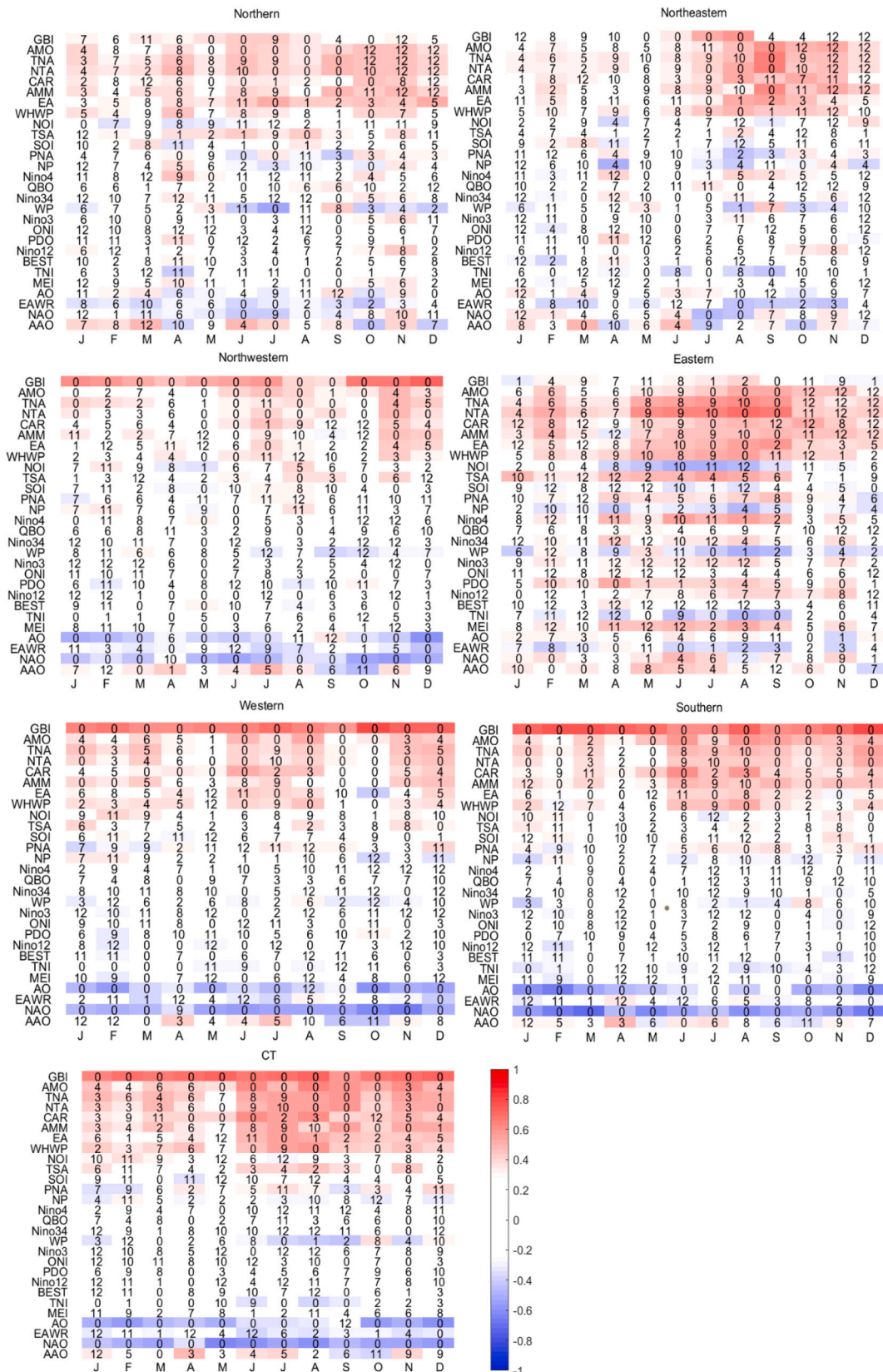


Fig. 4. Teleconnection relationships between coastal Greenland's temperatures and climate indexes. Significant correlations ( $p < 0.05$ ) correspond to correlation coefficients that are larger (less) than 0.25 ( $-0.25$ ), which are represented by red (blue) colors. (For interpretation of the references to colour in this figure legend, the reader is referred to the web version of this article.)

the southeastern coastal region of the island has the hottest warming trend of  $0.83\text{ }^{\circ}\text{C decade}^{-1}$ ; in addition, the CT rises by  $0.28\text{ }^{\circ}\text{C decade}^{-1}$ .

As shown in Fig. 2e, the mean annual coastal CT during 1952–2017 is  $-4.82\text{ }^{\circ}\text{C}$  (remaining steady compared with the mean temperature during the period 1981–2010), and there exists little difference in the mean annual coastal temperatures ( $0.94\text{--}1.36\text{ }^{\circ}\text{C}$ ) between the eastern and western regions. From the order of the climate tendency rate ( $\text{SE} > \text{N} > \text{NE} > \text{SW} > \text{NW} > \text{S}$ ), most regions display a warming temperature trend, but the temperature in the southern region shows no obvious change. In addition, the CT rises by  $0.23\text{ }^{\circ}\text{C decade}^{-1}$ .

From what has been discussed above, we can find that the coastal Greenland's temperature increases during 1952–2017 in most regions, but in most seasons, the southern region of the island experiences little change. The southeastern and northern regions are hotspots of warming, and the temperature in the eastern coastal region of the island changes more than that in the western region. The seasonal climate tendency rate exhibits large differences at different latitudes. Regarding the CT, winter displays the largest change rate ( $0.28\text{ }^{\circ}\text{C decade}^{-1}$ ), while the CT in summer increases by  $0.25\text{ }^{\circ}\text{C decade}^{-1}$ , and the CT in spring rises by  $0.17\text{ }^{\circ}\text{C decade}^{-1}$  with less variation.

Fig. 2f shows the inland temperature variation during the period 1997–2017. We can see that the inland temperature reaches a maximum value of  $-20.71\text{ }^{\circ}\text{C}$  in 2016 and a minimum value of  $-24.15\text{ }^{\circ}\text{C}$  in 2015. With regard to the climate tendency rate, the temperature has displayed an increasing trend over the past 21 years with a rate of increase of  $0.13\text{ }^{\circ}\text{C decade}^{-1}$ . The annual inland temperature has exhibited the same change trend as the coastal temperature, indicating that the temperature in Greenland has indeed increased during the period 1997–2017.

#### 4.2. Coastal temperature changes in the past 5 years (2013–2017) in Greenland

The Z values calculated by the M-K test are shown in Fig. 3. From the blue bars in Fig. 3a, we can see that the coastal spring temperature has significantly increased in most regions, reaching the significance threshold of 1.96 in every region except the northwestern, southwestern and southern regions. The temperatures in the northwestern and southern regions have remained steady, while that in the southwestern region shows a nonsignificant increasing trend.

The  $Z_{2017}$  values shown in Fig. 3b all pass the significance test, indicating remarkably strong warming in summer during 1952–2017.

As confirmed in Fig. 3c, there exists a prominent warming trend in every coastal region of the island during 1952–2017 except the southwestern and southern regions; however, the coastal autumn temperatures in these two regions increase only slightly and do not pass the significance test.

According to Fig. 3d, similar to autumn, the coastal winter temperatures in most regions increase significantly during 1952–2017, but the southern and southwestern regions exhibit nonsignificant increasing trends.

We also used the M-K method to test the significance of the coastal annual temperature change trends shown in Fig. 3e; the results indicate that most regions display a significant warming trend during 1952–2017 except for the southern region, the  $Z_{2017}$  value of which is statistically nonsignificant.

As Fig. 3 shows,  $\Delta Z$  is positive during the period 2013–2017 in most regions and seasons, indicating a rising temperature change trend in the last five years. The annual CT shows an increase of  $0.96\text{ }^{\circ}\text{C}$  during the period 2013–2017 relative to the 1981–2010 baseline.

Concerning the different regions, the temperatures in the northeastern and northern regions display faster warming trends than the other regions in most seasons except spring, whereas the temperature change trends in the southwestern, northwestern and southern regions of the island are relatively small. Regarding the seasonal temperature

change trend, the temperature changes in winter and spring are smaller than those in the other seasons. The change in the CT decreases in the following order: annual > autumn > summer > winter > spring.

#### 4.3. Teleconnection relationships between the coastal Greenland's temperature and climate indexes

As seen from Fig. 4, in the northern region of the island, the Atlantic climate indexes, including the GBI, AMO, TNA, NTA, CAR, AMM, EA and WHWP, exhibit strong positive correlations with temperature in most months with time lags of 0–12 months, except in February and May. The Atlantic climate indexes and temperature show a weak correlation in February and May. It should be noted that the GBI has a nonsignificant correlation with the winter temperature in the northern region. Additionally, significant negative correlations between the climate indexes and temperature are found for the NOI, WP, AO, EAWR and NAO. For the NOI, there exists a significant negative correlation in April and May with a time lag of 8–9 months. The WP passes the significance test in June and July and from October to January with a time lag of 0–11 months. For the AO, the correlation is prominent from April to July with a time lag of 0–9 months. For the EAWR, it is evident that in most months except December, the correlation passes the significance test at a level of 0.05 with a time lag of 0–10 months. The NAO has a significant negative correlation with temperature in most seasons with a time lag of 0–11 months, except in winter. It is obvious that the ENSO indexes, such as the MEI, BEST, Nino3, Nino4, Nino12, Nino3.4, ONI and SOI, have weak correlations with the temperature in the northern region, as these indexes do not pass the significance test.

In the northwestern region of the island, the GBI has a prominent positive correlation with temperature throughout the year without a time lag, and the other Atlantic climate indexes exhibit a significant positive correlation with temperature in summer, November and December with time lags of 0–12 months. However, the AO, EAWR, NAO and WP show prominent negative correlations with temperature; there exist no time lags between the AO and NAO and the coastal temperature, while the time lag between the EAWR and temperature is 0–2 months. The WP has a significant negative correlation with the winter temperature with a time lag of 2–12 months. Moreover, the ENSO indexes have no influence on the temperature in the northwestern region of the island.

Regarding the northeastern region of the island, temperature has the strongest positive correlations with the AMO, TNA, NTA, CAR, AMM, EA and WHWP in most seasons with time lags of 0–12 months, except in spring. This is different from the GBI, which shows a significant positive correlation with temperature in summer without a time lag. In contrast, the PNA, NP, WP, TNI, EAWR and NAO have significant negative correlations with temperature in autumn and at the end of summer with time lags of 0–9 months. The ENSO indexes have little influence on the temperature in this region, which is similar to the northern and northwestern regions.

In the southwestern region of the island, it is apparent that the GBI has a significant positive correlation with temperature throughout the year without a time lag, which is in accordance with the correlation in the northwestern region of the island. The other Atlantic climate indexes (AMO, TNA, NTA, CAR, AMM, EA and WHWP) have significant positive correlations with temperature in most months (except in April, May, September and October) with time lags of 0–10 months. Furthermore, the AO and NAO have significant negative correlations with temperature without a time lag.

From what can be seen in the southern region of the island, the correlations are similar to those in the western region. Significant positive correlations are observed between the Atlantic climate indexes and temperature in most months except February, April and May, and there are no time lags between the GBI and AMO and the temperature, while the time lags of the other climate indexes range from 0 to 11 months. There are also negative correlations between the AO and

NAO and the temperature without a time lag.

In the southeastern region of the island, the Atlantic climate indexes have significant positive correlations with temperature in most months with a time lag of 0–12 months, except in January, April and May. However, this region exhibits different behavior from the other regions insomuch that the ENSO indexes in this region show significant positive correlations with temperature in May through September with a time lag of 0–12 months. In addition, the NP, WP, TNI and EAWR have significant negative correlations with temperature from May to September with a time lag of 0–12 months.

We also analyzed the influences of the climate indexes on the CT. As shown in Fig. 4, the Atlantic climate indexes (GBI, AMO, TNA, NTA, CAR, AMM, EA and WHWP) exhibit significant positive correlations with temperature in most months, except in May. The GBI has no time lag, while the time lags of the other climate indexes range from 0–11 months. The WP, TNI, AO, EAWR and NAO show significant negative correlations with temperature, and the influences of the WP and TNI range mainly from July to September.

In summary, coastal Greenland's temperatures are influenced mainly by two sea currents, namely, the Arctic Ocean and Atlantic Ocean sea currents, due to the position of the island. In contrast, the ENSO indexes have little influence on the coastal temperatures. It is obvious that the GBI, AMO, TNA, NTA, CAR, AMM, EA and WHWP have significant positive correlations with temperature in most months, except in February and May. However, the NAO, AO and EAWR show significant negative correlations with temperature, and there exists a time lag effect for all the climate indexes (except for the GBI, AO and NAO).

#### 4.4. Sensitivity analysis of variables to coastal Greenland's temperatures

In Fig. 5, the larger the proportion of the variable is within the circle, the greater the influence of the variable on the coastal temperature. We can see that the GBI, NAO, CO<sub>2</sub>, AMO, N<sub>2</sub>O, SF<sub>6</sub>, CH<sub>4</sub>, and NOI are the most important variables that influence changes in the CT, indicating that both the effects of the atmospheric circulation indexes

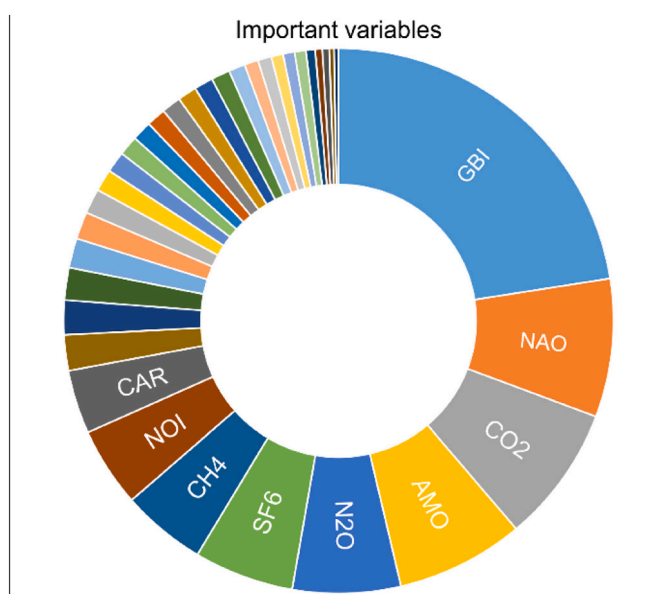


Fig. 5. Sensitivities of the influencing factors calculated by the random forest model. Large-scale climate indexes and GHGs were selected to determine the important factors influencing changes in the composite temperature, and all variables span the period from 1979 to 2017. The random forest model was used, which can explain 59.04% of the variance in the composite temperature. The mean error, root-mean-square error and R<sup>2</sup> of the model are -0.00371, 0.78 and 0.57, respectively, indicating a good fitting result.

and the effects of GHGs on temperature are important, which is in accordance with the findings of previous studies (Hanna et al., 2012; Chylek et al., 2009; Box et al., 2019). However, our findings differ in that the effect of the NOI on temperature is also important, although this index has a smaller effect on the CT than the other indexes mentioned in this section. This means that the CT may be influenced by biophysical indicators.

#### 4.5. Contribution rates of climate indexes and GHGs to coastal temperature change

In this section, we used multiple linear regression to calculate the contribution rates of important variables to Greenland's temperatures during the period 1979–2017. Fig. 6 shows the correlations between variables, which was used to choose variables to build stepwise regression equation (see method section 2.4), and finally, the multiple linear regression equation employed is as follows:  $CT = 1.586 * GBI + 0.016 * CO_2 + 0.156 * NOI + 0.043$ , which explains 78.2% of the variance in the CT. We divided the CT data and variables into two periods, namely, 1979–1998 and 1999–2017, to calculate the contribution rates of changes in different variables to the changes in the CT. The average temperature anomaly during 1999–2017 was 1.65 °C higher than that during 1979–1998. We calculated the contribution rates of changes in the GBI, CO<sub>2</sub> and NOI to the CT variation, and the results are 47.30%, 35.68%, and 17.02%, respectively, which indicates that both large-scale climate indexes and GHGs influence changes in coastal Greenland's temperatures.

#### 4.6. Discussion

The Arctic Monitoring and Assessment Programme (AMAP) Climate Change Update 2019 indicated that the average annual temperature in the Arctic increased 2.4 times faster than the average annual temperature in the Northern Hemisphere during the period 1971–2017. This temperature increase is still accelerating, and the average annual temperature during the period 2014–2018 was the warmest five years since 1900. The average annual temperature during the period 1971–2017 increased by 2.7 °C, and the average annual temperatures in the cold and warm seasons increased by 3.1 and 1.8 °C, respectively (Arctic Monitoring and Assessment Programme, 2019). In our study, the average annual temperature in coastal Greenland maintained an increasing trend in 2013–2017 and increased 0.96 °C relative to the 1981–2010 baseline, which is consistent with the results of AMAP reports. Temperature increases can lead to a series of problems, such as reductions in the area of sea ice, sea level rise, increasing ocean acidification and frequent extreme events, which threaten the safety of people's lives and property (World Meteorological Organization, 2019). Therefore, it is important to determine the reasons influencing temperature changes to keep the temperature increase before 2100 below 1.5 °C.

As mentioned above, the GBI, NAO, AMO and GHGs are important variables influencing the changes in coastal Greenland's temperatures. In this section, we will discuss the changes in these variables in recent years to explain why Greenland's temperatures have increased. We will also discuss the influence of decreasing sea ice on temperature change, as this reduction has a feedback effect on temperature (Screen and Francis, 2016).

The blocking index (BI) is an index corresponding to an anticyclonic high-pressure block (Rex, 1950) that is determined by the vortex gradient, and blocks form more easily in high-latitude regions (Li and Luo, 2019). When a block occurs, it is easier to maintain the block with a smaller vortex gradient. A block usually persists for 5 or more days (Häkkinen et al., 2011). In this section, we discuss the change in the BI over Greenland. From Section 4.5, we can find that the GBI has a positive correlation with temperature, and this relationship is in accordance with the findings of previous studies (Overland et al., 2015;

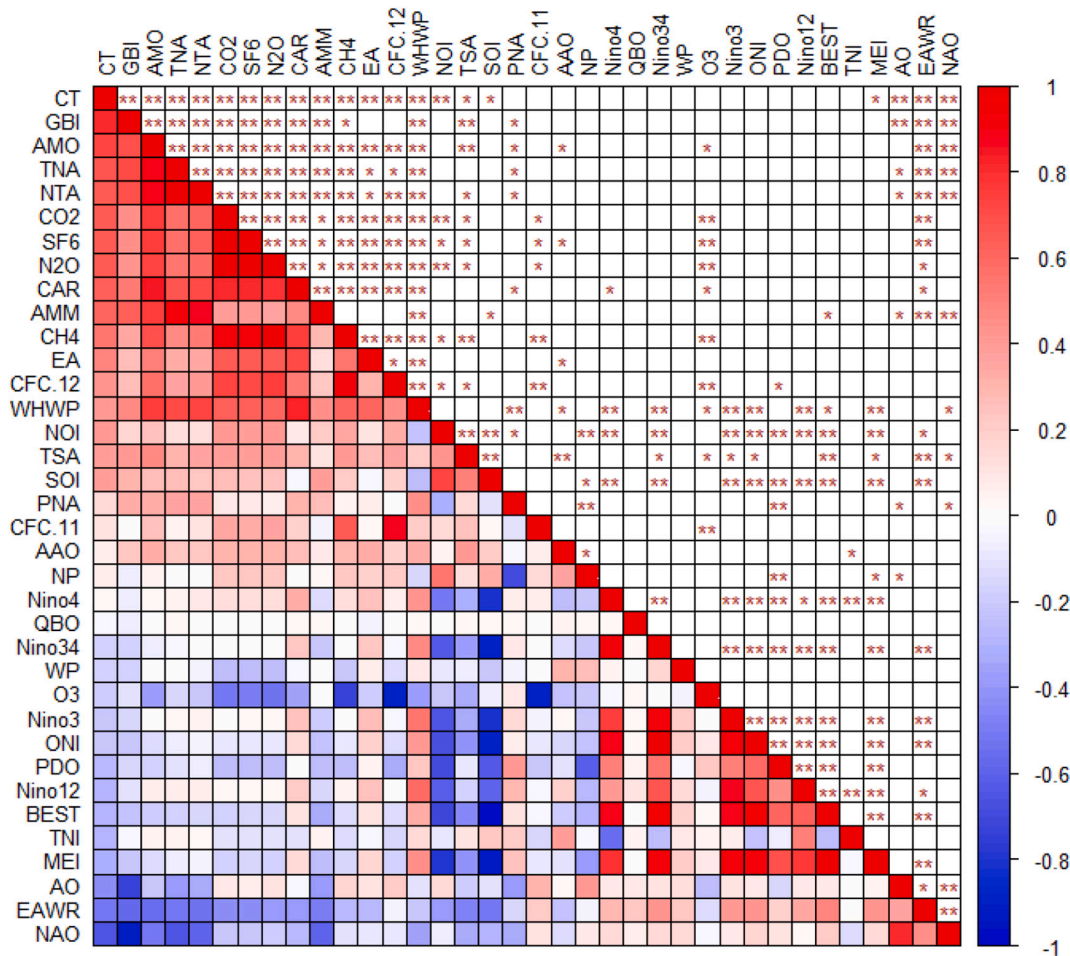


Fig. 6. Correlations between variables. \* and \*\* represent variables that are significant at significance levels of 0.05 and 0.01, respectively. And six variables were selected to build the multiple linear regression equation using stepwise regression method, namely, GBI, CO<sub>2</sub>, NOI, SOI, TSA and MEI.

Ballinger et al., 2018). When a block occurs, the air mass is trapped along an equatorward anticyclonic pressure ridge, and as a result, the high-latitude jet stream meanders (Häkkinen et al., 2011), leading to a temperature increase in the blocking region. On the other hand, as the temperature increases, the geopotential height is expanded and raised by the presence of warm air, leading to an increased intensity and frequency of high pressure, which correspondingly raises the rate of temperature increase (Hanna et al., 2015). As shown in Fig. 7a, the GBI has a nonsignificant increasing trend during the period 1952–2017, but the change in the Z value (Fig. 7c) is greater than zero during the period 2013–2017, indicating that the GBI increased over these five years, which may have contributed to the warming during the period 2013–2017, although the specific mechanism is unknown. Some researchers found that there exists a short-period negative correlation between the GBI and NAO (Woollings et al., 2008; Overland et al., 2012; Hanna et al., 2015) and a long-period positive correlation between the GBI and AMO (Häkkinen et al., 2013; Polyakov et al., 2005).

The NAO is the main mode of large-scale circulation in the North Atlantic and may influence the temperature variability therein (Barnston and Livezey, 1987; Hurrell, 1995). Many studies linked warming to the negative trend of the NAO, which is caused by anomalous Rossby wave-train activity from the tropical Pacific (Ding et al., 2014). This Rossby wave activity influences the temperature by transporting and accumulating heat by atmospheric warming through the water flux from the North Atlantic Ocean to Greenland (Straneo and Heimbach, 2013). From Fig. 7a, we can find that the durations of the positive and negative phases of the NAO are nearly equal during 2013–2017, which may have contributed little to the overall

temperature increase, but the NAO exhibits a minimum value in 2010, which may have contributed to the observed warming due to the time lag effect. Feldstein and Lee (2014) found that the accelerating loss of sea ice may have obscured the effect of the NAO on warming in recent years.

The AMO is another leading low-frequency mode in the Atlantic Ocean and is considered an important variable that results in warming (Chylek et al., 2009; Arguez et al., 2009). When the subtropical ocean warms (Levitus et al., 2012) and the AMO is in a warm phase, warm water will be transported to the subpolar region of the North Atlantic by persistent wind patterns, which may contribute to the warming of the subpolar region (Straneo and Heimbach, 2013). As shown in Fig. 7a, the AMO has always been in a positive phase since 1997, and from the M-K test results (Fig. 7c), the change in the Z value during 2013–2017 is greater than 0, indicating that the AMO increased in the last five years, which is likely to have contributed to the warming of Greenland.

Some scholars believe that the rapid warming of the Arctic is largely attributed to the greenhouse effect (Tabari and Talaei, 2011; Overland et al., 2019). The energy within the Earth system comes from solar radiation, and objects at the surface reflect some energy back into the atmosphere at the same time that they receive energy following the law of conservation of energy. GHGs play an important role in maintaining this balance of energy, as these gases can absorb some energy from longwave radiation scattered by objects, thereby keeping the Earth warm. However, when the concentrations of GHGs increase abnormally, more energy will be stored near the surface of the Earth, leading to warming of the air temperature. As shown in Fig. 7b, the concentrations of GHGs (CO<sub>2</sub>, CH<sub>4</sub>, N<sub>2</sub>O and SF<sub>6</sub>) have increased

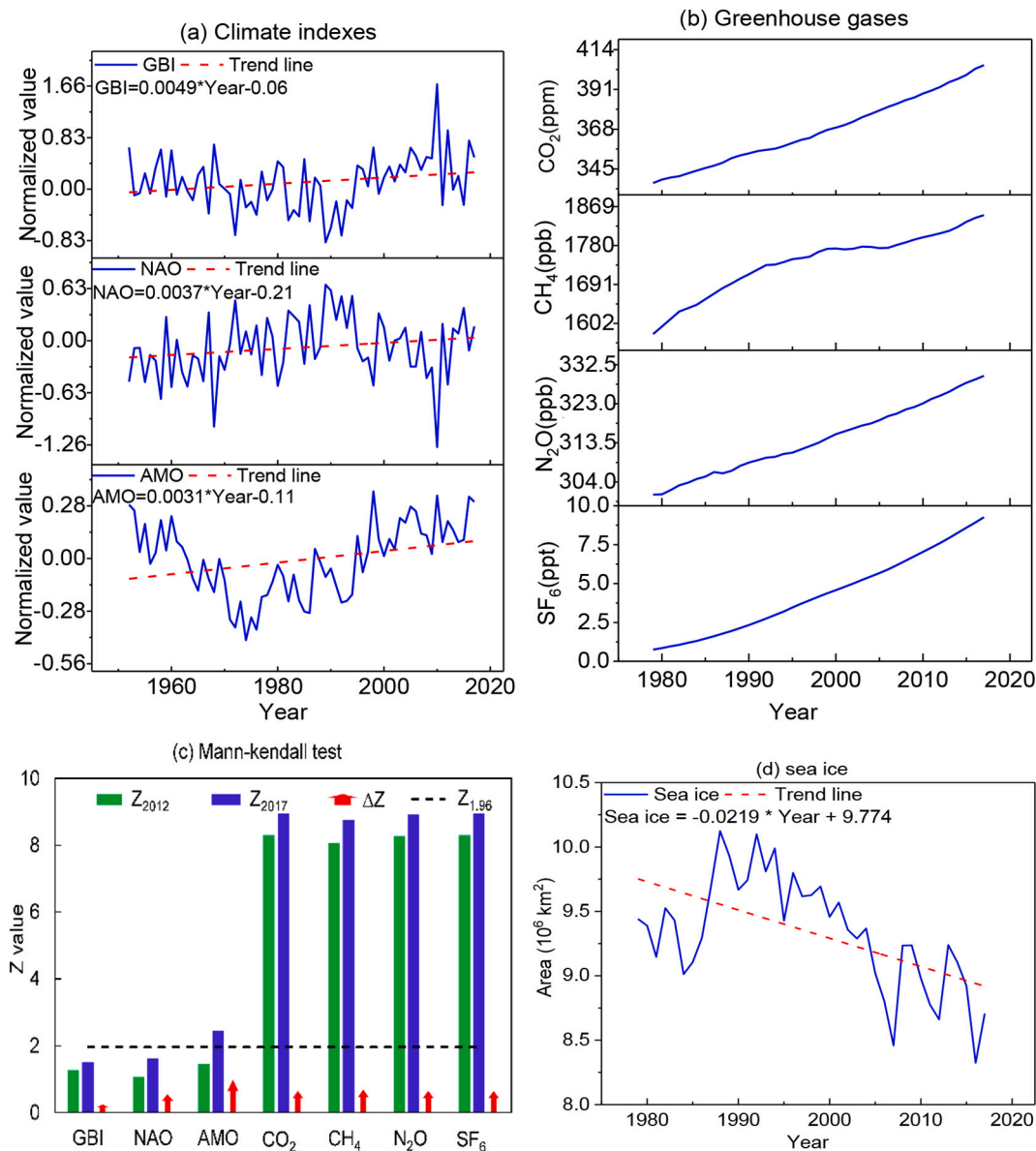


Fig. 7. Changes in important variables during the period 1952–2017.

significantly since 1979; despite policies intended to cut emissions, the concentration of  $CO_2$  is still higher than the preindustrial revolution level (approximately 280 ppm). These increases in GHGs have contributed to the warming of Greenland. As the main greenhouse gas,  $CO_2$  plays a leading role in global warming;  $CO_2$  accounts for approximately 80% of warming compared with other GHGs, such as  $CH_4$ ,  $N_2O$  and CFCs (Lashof and Ahuja, 1990). From Section 4.5, we know that the contribution rate of  $CO_2$  to coastal Greenland's temperature change is 35.68%; thus,  $CO_2$  was the main contributor to the warming of Greenland.

Increasing temperatures will lead to further sea ice loss, but a reduction in sea ice also contributes to global warming due to sea ice albedo feedback (Screen and Simmonds, 2010; Meier et al., 2014). The absorption of surface radiation will increase after an increase in sea ice reduction because the sea ice albedo decreases and the amount of evaporation from the ocean increases, leading to the additional formation of low-lying clouds and atmospheric water, which changes the transport of heat and water fluxes from the ocean to other regions (Praetorius et al., 2018; Graversen et al., 2008). Fig. 7d shows the change in the sea ice area during the period 1979–2017 in the Northern

Hemisphere. We can see that sea ice decreased at a rate of  $219,000\ km^2\ decade^{-1}$ , and it reached the lowest value of  $8,325,000\ km^2$  in 2016, which means that more heat and water will be transported to Greenland, contributing to the warming of Greenland.

In reality, changes in temperature are influenced by many variables simultaneously. We analyzed only the most important variables influencing temperature, but the specific mechanism responsible for these changes is complex and remains unknown. In the future, we will focus on the interaction between the ocean and atmosphere to interpret how ocean-atmosphere processes contribute to the warming of Greenland. Therefore, it will be necessary to study the Greenland ice sheet and sea ice as a whole (Xiao et al., 2019). The results can serve as references for climate prediction and Greenland ice sheet monitoring.

### 5. Conclusions

Three-quarters of Greenland is located within the Arctic circle, and the temperature change of the Arctic is twice the change in the global temperature. As 82% of the island is covered by an ice sheet, Greenland plays an important role in sea level rise. The study of temperature

change can provide a reference for Greenland ice sheet mass balance calculations.

In this study, we analyzed the seasonal and annual coastal temperature changes during the period 1952–2017, and we focused mainly on the temperature changes over the last five years of this period. Overall, the values of  $\Delta Z$  obtained from M-K tests are greater than 0 in different seasons and regions during the period 2013–2017, indicating a consistent warming trend over the last five years. The CT increased by 0.96 °C relative to the 1981–2010 baseline in this period. We also analyzed the inland annual temperature change trend during the period 1997–2017, revealing an increase of 0.13 °C decade<sup>-1</sup>, which is the same change trend as the trend of the coastal temperature change.

Twenty-eight large-scale climate-ocean indexes and six GHGs were selected to determine the most important variables influencing these temperature changes. The random forest model and Pearson correlation analysis both showed a high degree of consistency; the GBI, NAO, CO<sub>2</sub>, AMO, N<sub>2</sub>O, SF<sub>6</sub>, CH<sub>4</sub>, and NOI are the most important variables influencing the changes in the CT.

Finally, we calculated the contribution rates of the most important variables to the coastal temperature change during the period 1979–2017 using multiple linear regression; the contribution rates of the GBI, CO<sub>2</sub> and NOI to temperature change in Greenland are 47.30%, 35.68%, and 17.02%, respectively.

## Declaration of Competing Interest

None.

## Acknowledgments

This study was supported by the Second Tibetan Plateau Scientific Expedition and Research Program (No.2019QZKK0405), the National Key Research and Development Program of China (No. 2018YFE0196000), and the National Natural Science Foundation of China (No. 51879009).

## References

- Abdalati, W., Steffen, K., 1997. Snowmelt on the Greenland Ice Sheet as derived from passive microwave satellite Data. *J. Clim.* 10 (2), 165–175. [https://doi.org/10.1175/1520-0442\(1997\)010<0165:SOTGIS>2.0.CO;2](https://doi.org/10.1175/1520-0442(1997)010<0165:SOTGIS>2.0.CO;2).
- Arctic Monitoring and Assessment Programme, 2019. AMAP climate change update 2019: An update to key findings of snow. In: *Water, Ice and Permafrost in the Arctic (SWIPA) 2017. Arctic Monitoring and Assessment Programme (AMAP)*.
- Arguez, A., O'Brien, J.J., Smith, S.R., 2009. Air temperature impacts over Eastern North America and Europe associated with low-frequency North Atlantic SST variability. *Int. J. Climatol.* 29, 1–10. <https://doi.org/10.1002/joc.1700>.
- Ballinger, T.J., Hanna, E., Hall, R.J., Cropper, T.E., Miller, J., Ribergaard, M.H., Overland, J.E., Hoyer, J.L., 2018. Anomalous blocking over Greenland preceded the 2013 extreme early melt of local sea ice. *Ann. Glaciol.* 59 (76pt2), 181–190. <https://doi.org/10.1017/aog.2017.30>.
- Barnston, A.G., Livezey, R.E., 1987. Classification, seasonality and persistence of Low-frequency atmospheric circulation patterns. *Mon. Weather Rev.* 115 (6), 1083–1126. [https://doi.org/10.1175/1520-0493\(1987\)115<1083:CSAPOL>2.0.CO;2](https://doi.org/10.1175/1520-0493(1987)115<1083:CSAPOL>2.0.CO;2).
- Box, J.E., 2002. Survey of Greenland instrumental temperature records: 1873–2001. *Int. J. Climatol.* 22 (15), 1829–1847. <https://doi.org/10.1002/joc.852>.
- Box, J.E., Yang, L., Bromwich, D.H., Bai, L.S., 2009. Greenland ice sheet surface air temperature variability: 1840–2007. *J. Clim.* 22 (14), 4029–4049. <https://doi.org/10.1175/2009JCLI2816.1>.
- Box, J.E., Colgan, W.T., Røjle Christensen, T., Schmidt, N.M., Lund, M., Parmentier, F.-J.W., Brown, R., Bhatt, U.S., Euskirchen, E.S., Romanovsky, V.E., Walsh, J.E., Overland, J.E., Wang, M., Corell, R.W., Meier, W.N., Wouters, B., Mernild, S., Mård, J., Pawlak, J., Skovgård Olsen, M., 2019. Key indicators of Arctic climate change: 1971–2017. *Environ. Res. Lett.* 14. <https://doi.org/10.1088/1748-9326/aaef1b>.
- Breiman, L., 2001. Random forests. *Mach. Learn.* 45 (1), 5–32. <https://doi.org/10.1023/A:1010933404324>.
- Chylek, P., Box, J.E., Lesins, G., 2004. Global warming and the Greenland ice sheet. *Clim. Chang.* 63 (1–2), 201–221. <https://doi.org/10.1023/B:CLIM.0000>.
- Chylek, P., Folland, C.K., Lesins, G., Dubey, M.K., Wang, M., 2009. Arctic air temperature change amplification and the Atlantic Multidecadal Oscillation. *Geophys. Res. Lett.* 36 (14), L14801. <https://doi.org/10.1029/2009GL038777>.
- Cuffey, K., Marshall, S.J., 2000. Substantial contribution to sea-level rise during the last interglacial from the Greenland ice sheet. *Nature* 404, 591–594. <https://doi.org/10.1038/35007053>.
- Ding, Q., Wallace, J.M., Battisti, D.S., Steig, E.J., Gallant, A.J.E., Kim, H.-J., Geng, L., 2014. Tropical forcing of the recent rapid Arctic warming in northeastern Canada and Greenland. *Nature* 509, 209–212. <https://doi.org/10.1038/nature13260>.
- Feldstein, S.B., Lee, S., 2014. Intraseasonal and interdecadal jet shifts in the Northern Hemisphere: the role of warm pool tropical convection and sea ice. *J. Clim.* 27 (17), 6497–6518. <https://doi.org/10.1175/JCLI-D-14-00057.1>.
- Graversen, R., Mauritsen, T., Tjernström, M., Källén, E., Svensson, G., 2008. Vertical structure of recent Arctic warming. *Nature* 541, 53–56. <https://doi.org/10.1038/nature06502>.
- Häkkinen, S., Rhines, P.B., Worthen, D.L., 2011. Atmospheric blocking and Atlantic multidecadal ocean variability. *Science* 334 (6056), 655–659. <https://doi.org/10.1126/science.1205683>.
- Häkkinen, S., Rhines, P.B., Worthen, D.L., 2013. Northern North Atlantic Sea surface height and ocean heat content variability. *J. Geophys. Res. Oceans* 118 (7), 3670–3678. <https://doi.org/10.1002/jgrc.20268>.
- Hanna, E., Cappelen, J., 2003. Recent cooling in coastal southern Greenland and relation with the North Atlantic Oscillation. *Geophys. Res. Lett.* 30 (3), 1132. <https://doi.org/10.1029/2002GL015797>.
- Hanna, E., Mernild, S.H., Cappelen, J., Steffen, K., 2012. Recent warming in Greenland in a long-term instrumental (1881–2012) climatic context: I. Evaluation of surface air temperature records. *Environ. Res. Lett.* 7 (4), 045404. <https://doi.org/10.1088/1748-9326/7/4/045404>.
- Hanna, E., Cropper, T.E., Jones, P.D., Scaife, A.A., Allan, R., 2015. Recent seasonal asymmetric changes in the NAO (a marked summer decline and increased winter variability) and associated changes in the AO and Greenland Blocking Index. *Int. J. Climatol.* 35 (9), 2540–2554. <https://doi.org/10.1002/joc.4157>.
- Hanna, E., Cropper, T.E., Hall, R.J., Cappelen, J., 2016. Greenland Blocking Index 1851–2015: a regional climate change signal. *Int. J. Climatol.* 36 (15), 4847–4861. <https://doi.org/10.1002/joc.4673>.
- Hidalgo-Muñoz, J.M., Gámiz-Fortis, S.R., Castro-Díez, Y., Argüeso, D., Esteban-Parra, M.J., 2015. Long-range seasonal streamflow forecasting over the Iberian Peninsula using large-scale atmospheric and oceanic information. *Water Resour. Res.* 51 (5), 3543–3567. <https://doi.org/10.1002/2014WR016826>.
- Hurrell, J.W., 1995. Decadal trends in the North Atlantic Oscillation: regional temperatures and precipitation. *Science* 269 (5224), 676–679. <https://doi.org/10.1126/science.269.5224.676>.
- Hvidberg, C., 2000. When Greenland ice melts. *Nature* 404 (6778), 551–552. <https://doi.org/10.1038/35007164>.
- Johannessen, O.M., BenCTsson, L., Miles, M.W., Kuzmina, S.I., Semenov, V.A., Alekseev, G.V., Nagurnyi, A.P., Zakharov, V.F., Bobylev, L.P., Pettersson, L.H., Hasselmann, K., Cattle, H.P., 2004. Arctic climate change: observed and modelled temperature and sea-ice variability. *Tellus A* 56 (4), 328–341. <https://doi.org/10.1111/j.1600-0870.2004.00060.x>.
- Kendall, M.G., 1948. *Rank Correlation Methods*. Griffin, London.
- Lashof, D.A., Ahuja, D.R., 1990. Relative contributions of greenhouse gas emissions to global warming. *Nature* 344, 529–531. <https://doi.org/10.1038/344529a0>.
- Levitius, S., Antonov, J.I., Boyer, T.P., Baranova, O.K., Garcia, H.E., Locarnini, R.A., Mishonov, A.V., Reagan, J.R., Seidov, D., Yarosh, E.S., Zweng, M.M., 2012. World Ocean heat content and thermocline sea level change (0–2000 m), 1955–2010. *Geophys. Res. Lett.* 39 (10), L10603. <https://doi.org/10.1029/2012GL051106>.
- Li, M., Luo, D., 2019. Winter Arctic warming and its linkage with midlatitude atmospheric circulation and associated cold extremes: the key role of meridional potential vorticity gradient. *China Earth Sci.* 62. <https://doi.org/10.1007/s11430-018-9350-9>.
- Liaw, A., Wiener, M., 2002. Classification and Regression by randomForest. *R News* 2/3 (1609–3631), 18–22.
- Mann, H.B., 1945. Nonparametric test against trend. *Econometrica* 13 (3), 245–259.
- Meier, W.N., Hovelsrud, G.K., Van Oort, B.E.H., Key, J.R., Kovacs, K.M., Michel, C., Haas, C., Granskog, M.A., Gerland, S., Perovich, D.K., Makshtas, A., Reist, J.D., 2014. Arctic Sea ice in transformation: a review of recent observed changes and impacts on biology and human activity. *Rev. Geophys.* 52 (3), 185–217. <https://doi.org/10.1002/2013RG000431>.
- Mernild, S.H., Hanna, E., Yde, J.C., Cappelen, J., Malmros, J.K., 2014. Coastal Greenland air temperature extremes and trends 1890–2010: annual and monthly analysis. *Int. J. Climatol.* 34 (5), 1472–1487. <https://doi.org/10.1002/joc.3777>.
- Mestas-Nunez, A.M., Enfield, D.B., 2001. Eastern equatorial Pacific SST variability: ENSO and Non-ENSO components and their climatic associations. *J. Clim.* 14 (3), 391–402. [https://doi.org/10.1175/1520-0442\(2001\)014<0391:EEPSVE>2.0.CO;2](https://doi.org/10.1175/1520-0442(2001)014<0391:EEPSVE>2.0.CO;2).
- Mitchell, J.M., Dzerdzevskii, B., Flohn, H., Hofmeyr, W.L., Lamb, H.H., Rao, K.N., Wallén, C.C., 1966. *Climate Change*. WMO Publ.
- Overland, J.E., Francis, J.A., Hanna, E., Wang, M., 2012. The recent shift in early summer Arctic atmospheric circulation. *Geophys. Res. Lett.* 39 (19), L19804. <https://doi.org/10.1029/2012GL03268>.
- Overland, J.E., Francis, J., Hall, R., Hanna, E., Kim, S.-J., Vihma, T., 2015. The melting Arctic and mid-latitude weather patterns: are they connected? *J. Clim.* 28 (20), 7917–7932. <https://doi.org/10.1175/JCLI-D-14-00822.1>.
- Overland, J., Dunlea, E., Box, J.E., Corell, R., Forsius, M., Kattsov, V., Olsen, M.S., Pawlak, J., Reiersen, L.-O., Wang, M., 2019. The urgency of Arctic change. *Polar Sci.* 21, 6–13. <https://doi.org/10.1016/j.polar.2018.11.008>.
- Penland, C., Matrosova, L., 1998. Prediction of tropical Atlantic Sea surface temperatures using Linear Inverse Modeling. *J. Clim.* 11 (3), 483–496. [https://doi.org/10.1175/1520-0442\(1998\)011<0483:POTASS>2.0.CO;2](https://doi.org/10.1175/1520-0442(1998)011<0483:POTASS>2.0.CO;2).
- Polyakov, I.V., Alekseev, G.V., Bekryaev, R.V., Bhatt, U., Colony, R.L., Johnson, M.A., Karklin, V.P., Makshtas, A.P., Walsh, D., Yulin, A.V., 2002. Observationally based assessment of polar amplification of global warming. *Geophys. Res. Lett.* 29 (18), 1878. <https://doi.org/10.1029/2001GL011111>.
- Polyakov, I.V., Bhatt, U.S., Simmons, H.L., Walsh, D., Walsh, J.E., Zhang, X., 2005.

- Multidecadal variability of North Atlantic temperature and salinity during the twentieth century. *J. Clim.* 18 (21), 4562–4581. <https://doi.org/10.1175/JCLI3548.1>.
- Praetorius, S., Rugenstein, M., Persad, G., Caldeira, K., 2018. Global and Arctic climate sensitivity enhanced by changes in North Pacific heat flux. *Nat. Commun.* 9, 3124. <https://doi.org/10.1038/s41467-018-05337-8>.
- Rex, D.F., 1950. Blocking action in the middle troposphere and its effect upon regional climate. *Tellus* 2 (4), 275–301. <https://doi.org/10.1111/j.2153-3490.1950.tb00339.x>.
- Schwing, F.B., Murphree, T., Green, P.M., 2002. The Northern Oscillation Index (NOI): a new climate index for the Northeast Pacific. *Prog. Oceanogr.* 53 (2–4), 115–139. [https://doi.org/10.1016/S0079-6611\(02\)00027-7](https://doi.org/10.1016/S0079-6611(02)00027-7).
- Screen, J.A., Francis, J.A., 2016. Contribution of sea-ice loss to Arctic amplification is regulated by Pacific Ocean decadal variability. *Nat. Clim. Chang.* 6, 856–860. <https://doi.org/10.1038/nclimate3011>.
- Screen, J.A., Simmonds, I., 2010. The central role of diminishing sea ice in recent Arctic temperature amplification. *Nature* 464, 1334–1337. <https://doi.org/10.1038/nature09051>.
- Statistics Greenland; (2018) Greenland in Figures 2018. 15th revised edition. Statistics Greenland 1–40.
- Steffen, K., Box, J.E., 2001. Surface climatology of the Greenland Ice Sheet: Greenland climate Network 1995–1999. *J. Geophys. Res.* 106 (D24), 33951–33964. <https://doi.org/10.1029/2001JD900161>.
- Steffen, K., Box, J.E., Abdalati, W., 1996. Greenland Climate Network: GC-Net. In: Colbeck, S.C. Ed (Ed.), *CRREL 96-27 Special Report on Glaciers, Ice Sheets and Volcanoes*, trib. to M. Meier, pp. 98–103.
- Straneo, F., Heimbach, P., 2013. North Atlantic warming and the retreat of Greenland's outlet glaciers. *Nature* 504, 36–43. <https://doi.org/10.1038/nature12854>.
- Tabari, H., Talaei, P.H., 2011. Analysis of trends in temperature data in arid and semi-arid regions of Iran. *Glob. Planet. Chang.* 79 (1–2), 1–10. <https://doi.org/10.1016/j.gloplacha.2011.07.008>.
- Vinther, B.M., Andersen, K.K., Jones, P.D., Briffa, K.R., Cappelen, J., 2006. Extending Greenland temperature records into the late eighteenth century. *J. Geophys. Res.* 111, D11105. <https://doi.org/10.1029/2005JD006810>.
- Woollings, T., Hoskins, B., Blackburn, M., Berrisford, P., 2008. A new Rossby wave-breaking interpretation of the North Atlantic Oscillation. *J. Atmos. Sci.* 65 (2), 609–626. <https://doi.org/10.1175/2007JAS2347.1>.
- World Meteorological Organization, 2018. *WMO Statement on the State of the Global Climate in 2017*. World Meteorological Organization (WMO).
- World Meteorological Organization, 2019. *The Global Climate in 2015–2019*. World Meteorological Organization (WMO).
- Xiao, C.D., Chen, Z.Q., Jiang, L.M., Ding, M.H., Dou, T.F., 2019. A study of monitoring, simulation and climate impact of Greenland Ice Sheet. *Adv. Earth Science* 34 (8), 781–786. <https://doi.org/10.11867/j.issn.1001-8166.2019.08.0781>.